ACS central science

http://pubs.acs.org/journal/acscii

Research Article

A Synthetic Gene Library Yields a Previously Unknown Glycoside Phosphorylase That Degrades and Assembles Poly-β-1,3-GlcNAc, Completing the Suite of β-Linked GlcNAc Polysaccharides

Spencer S. Macdonald, Jose H. Pereira, Feng Liu, Gregor Tegl, Andy DeGiovanni, Jacob F. Wardman, Samuel Deutsch, Yasuo Yoshikuni, Paul D. Adams, and Stephen G. Withers*

Cite This: https://doi.org/10.1021/acscentsci.1c01570

Read Online

ACCESS | Metrics & More | Article Recommendations | Supporting Information

ABSTRACT: The considerable utility of glycoside phosphorylases (GPs) has led to substantial efforts over the past two decades to expand the breadth of known GP activities. Driven largely by the increase of available genomic DNA sequence data, the gap between the number of sequences in the carbohydrate active enzyme database (CAZy DB) and its functionally characterized members continues to grow. This wealth of sequence data presented an exciting opportunity to explore the ever-expanding CAZy DB to discover new GPs with never-before-described functionalities. Utilizing an *in silico* sequence analysis of CAZy family GH94, we discovered and then functionally and structurally characterized the new GP β-1,3-*N*-acetylglucosaminide phosphorylase. This new GP was sourced from the genome of the cell-wall-less Mollicute bacterium, *Acholeplasma laidlawii* and was found to synthesize β-1,3-linked *N*-acetylglucosaminide linkages. The resulting poly-β-1,3-*N*-acetylglucosamine represents a new, previously undescribed biopolymer that completes the set of possible β-linked GlcNAc homopolysaccharides together with chitin (β-1,4) and PNAG (poly-β-1,6-*N*-acetylglucosamine). The new biopolymer was denoted *acholetin*, a combination of the genus *Acholeplasma* and the polysaccharide chitin, and the new GP was thus denoted acholetin phosphorylase (AchP). Use of the reverse phosphorolysis action of AchP provides an efficient method to enzymatically synthesize acholetin, which is a new biodegradable polymeric material.

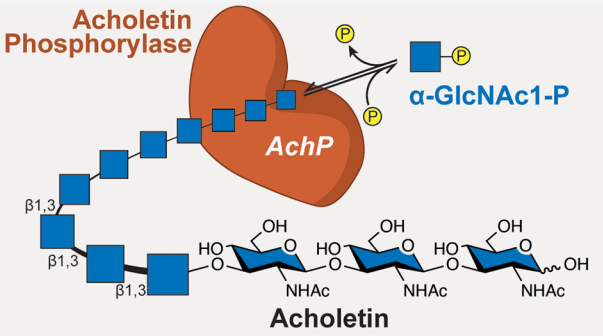

INTRODUCTION

Polysaccharides are the most abundant biopolymers on earth, play numerous key roles in living systems, and have been utilized to develop an extensive range of functional materials benefiting society.[1] The renewability and carbon neutrality of biosourced polysaccharides have led to significant interest in their potential to replace synthetic polymers, such as plastics, derived from fossil fuels.[2] Beyond being sustainable and environmentally friendly, poly- and oligosaccharides have seen considerable biomedical applications due to their favorable biocompatible and biodegradable properties.[3,4] They have been central in the development of nano- and microparticles for drug delivery systems,[5−11] glycan conjugated therapeutics,[12−14] wound dressings,[15−19] and scaffolds for tissue engineering and 3D bioprinting.[20−26] The diverse applications of poly- and oligosaccharides originate from the identities of their monomeric precursors and the types of glycosidic linkages that connect them. Based upon the large number of potential precursors and the array of possible linkages, polymeric carbohydrates are able to adopt a wide range of structures and functions, with greater conceivable complexity than their amino and nucleic acid counterparts. With this added complexity comes added difficulty when attempting to chemically synthesize poly- or oligosaccharides.[27] In the biomedical context, it is vital that synthesis occurs under conditions that result in a uniform and sequence-defined carbohydrate to achieve the desired properties of the functional material. However, due in large part to the more or less chemical equivalency of individual glycoside hydroxyl groups, chemical synthesis often requires multiple inefficient protection and deprotection steps to control the stereo- and regiochemical outcome of glycosylation reactions,[28] resulting in increased costs and diminished yields. Enzymatic synthesis represents an advantageous alternative to achieving uniform and sequence-defined carbohydrates by exploiting an enzyme's innate substrate specificity and conformational control, thereby

Received: December 22, 2021

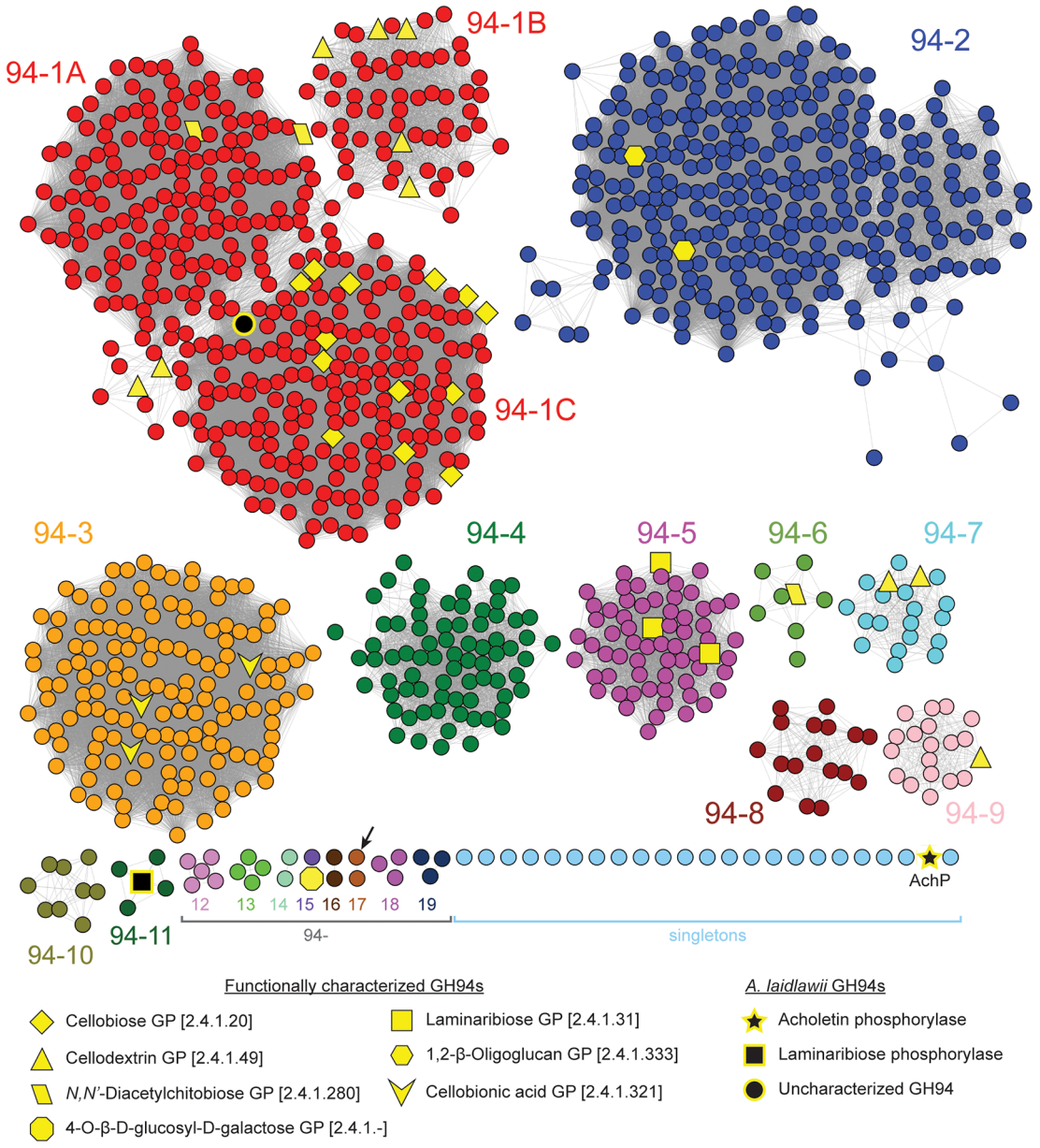

Figure 1. GH94 sequence similarity network. Amino acid SSN of 1161 unique GH94 sequences from the CAZy DB with an alignment score threshold of 10^{-200}. Sequence fragments below 200 amino acids and multidomain sequences greater than 600 amino acids were excluded. Nodes colored based on meta-node clustering. Functionally characterized GH94s are represented as yellow symbols with black outlines, and *A. laidlawii* GH94s are represented as black symbols with yellow outlines. The black arrow (meta-node 94-17) indicates the node with the lowest alignment score (1.1×10^{-175}) with AchP.

avoiding the inefficiencies associated with chemical synthesis.[28,29]

Glycoside phosphorylases (GPs) are a class of carbohydrate active enzymes (CAZy)[30] that have seen frequent use for poly- and oligosaccharide synthesis. GPs act through a process known as phosphorolysis that cleaves the glycosidic linkage with a phosphate molecule resulting in the release of a sugar 1-phosphate.[31,32] Due to the roughly equivalent free energies associated with the intersugar glycosidic linkage and the glycosyl phosphate bond of the released sugar 1-phosphate, GPs can perform phosphorolysis in reverse.[33] This allows GPs to be used for carbohydrate synthesis by adding glycosyl moieties from sugar 1-phosphates to suitable acceptors.[34] Furthermore, this synthetic paradigm is amenable to large-scale applications due to the relatively low cost associated with the sugar 1-phosphate starting materials. The innate substrate specificity and conformational control offered by GPs, together with their inexpensive starting materials, make these enzymes attractive tools for poly- and oligosaccharide synthesis. In some cases, GPs display broader specificity toward non-native substrate structures, allowing the assembly of a range of synthetic products. As new GP activities are discovered and the array of these useful biocatalysts continues to grow, the potential to generate novel and diverse carbohydrate-based materials constantly increases.

We report here the discovery and functional and structural characterization of a *β*-1,3-*N*-acetylglucosaminide phosphorylase, a new GP belonging to the CAZy family GH94. The new GP was sourced from the genome of the cell-wall-less Mollicute bacterium *Acholeplasma laidlawii* and was found to synthesize *β*-

https://doi.org/10.1021/acscentsci.1c01570
ACS Cent. Sci. XXXX, XXX, XXX−XXX

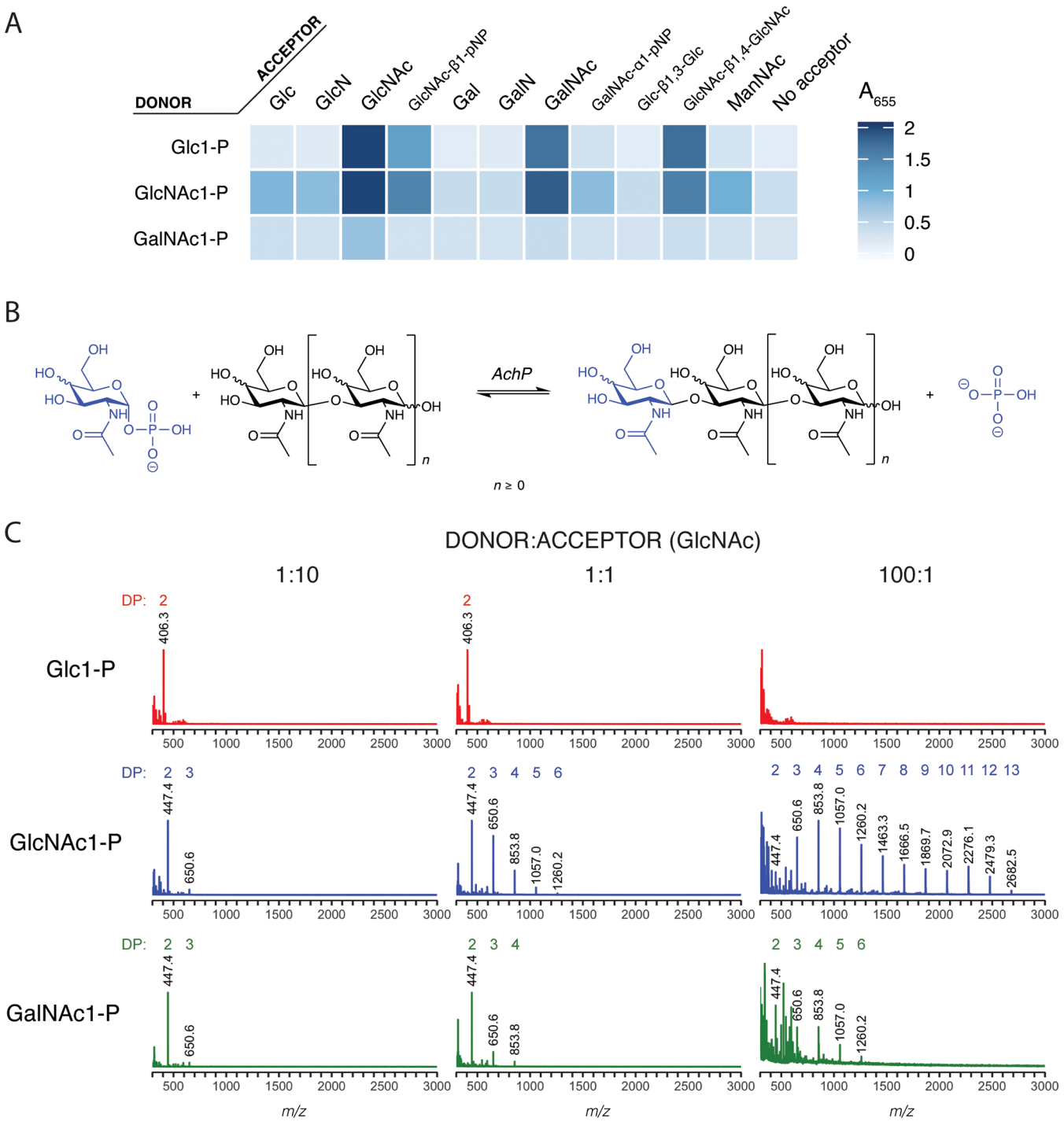

Figure 2. Functional characterization of AchP. (A) Purified AchP donor and acceptor specificity screen. AchP donor and acceptor specificity screen. Activity was monitored by coupling phosphate release from reverse phosphorolysis to the formation of molybdenum blue, which absorbs strongly at 655 nm. (B) AchP reaction scheme. (C) AchP degree of polymerization (DP) analysis. DP was characterized using MALDI-MS with donors Glc1-P, GlcNAc1-P, or GalNAc1-P and GlcNAc as the acceptor, in either 1:10, 1:1, or 100:1 donor-to-acceptor ratios. Peaks are labeled with their m/z (representing acholetin + Na adducts [M + Na]) and corresponding DP (colored number). The y-axis represents the relative signal intensity. DP analysis with GalNAc as the acceptor is shown in Figure S6.

1,3-linked *N*-acetylglucosamine (GlcNAc) linkages using the donor α-*N*-acetylglucosamine 1-phosphate (GlcNAc1-P). To our knowledge, the resulting poly-β-1,3-*N*-acetylglucosamine has not previously been described and therefore represents a new biopolymer. Furthermore, it completes the set of possible β-linked GlcNAc homopolysaccharides together with poly-β-1,4-*N*-acetyl-glucosamine, or chitin, the major component of arthropod exoskeletons and fungi cell walls and the second most abundant biopolymer on earth, and poly-β-1,6-*N*-acetylglucosamine (PNAG), a key virulence factor required for biofilm formation by numerous pathogenic bacteria. Poly-β-1,3-*N*-acetylglucosamine was denoted *acholetin*, a combination of the genus *Acholeplasma* and the well-known β-1,4-GlcNAc polysaccharide, chitin. Therefore, the new β-1,3-*N*-acetylgluco-

https://doi.org/10.1021/acscentsci.1c01570
ACS Cent. Sci. XXXX, XXX, XXX−XXX

Table 1. Reverse Phosphorolysis Kinetic Parameters for AchP[a]

substrate	donor	K_m (mM)	k_{cat} (s^{-1})	k_{cat}/K_m (mM^{-1} s^{-1})	K_i (mM)
GlcNAc	αGlcNAc1-P	3.5 ± 0.4	50.8 ± 3.2	14.5 ± 8.0	27.1 ± 3.6
	αGlc1-P	29.9 ± 3.7	24.2 ± 1.6	0.8 ± 0.4	281 ± 43
GalNAc	αGlcNAc1-P	71.4 ± 4.1	46.7 ± 0.9	0.7 ± 0.2	N/A
	αGlc1-P	164 ± 14	12.5 ± 0.5	0.08 ± 0.04	N/A

[a]Reactions were carried out with 10 mM GlcNAc1-P or Glc1-P donors and varying concentrations of either GlcNAc or GalNAc. Michaelis–Menten plots are shown in Figure S2.

saminide phosphorylase is referred to, hereafter, as acholetin phosphorylase (AchP).

RESULTS AND DISCUSSION

Acholetin phosphorylase (AchP) was discovered as part of a larger study aiming to characterize a gene synthesis library (prepared by the Joint Genome Institute) containing a phylogenomically diverse set of glycoside phosphorylases (GPs). A particular objective was to find phosphorylases that degrade chitin, since at present only *N*,*N*′-diacetylchitobiose phosphorylases are known. Such a chitin phosphorylase could be useful in large-scale conversion of waste chitin into useful biochemicals. The broader study targeted GPs across five carbohydrate active enzyme (CAZy) families, but for the specific purpose noted, we were most interested in members of GH94, the family that contains *N*,*N*′-diacetylchitobiose phosphorylases. To that end, an activity-based screen was performed looking for phosphate release from the sugar phosphate donor in the presence of various acceptors: most importantly for this purpose, GlcNAc and *N*,*N*′-diacetylchitobiose. Only 1 of the 18 GH94 enzymes screened yielded a strong hit with GlcNAc, and this was also the only one to transfer to *N*,*N*′-diacetylchitobiose (Figure S1). We therefore proceeded to investigate this lone hit in more detail, both through a detailed informatics analysis and through kinetic and mechanistic studies on purified enzyme.

Sequence Similarity Network. A sequence similarity network (SSN) was constructed to analyze the sequence diversity within the GH94 family to reveal the potential activity of AchP by determining whether it clustered with other functionally characterized GH94s (Figure 1). The SSN was constructed from a set of 1161 GH94 amino acid sequences with an *E*-value threshold of 10^{-200}, corresponding to a pairwise sequence identity of over 40%.[35−38] At the time of writing, the GH94 family contained seven known phosphorylase activities (Table S1) that are represented within 36 functionally characterized members. The overlaid functional annotations were based on the list of characterized GH94s in the CAZy DB[30] (www.cazy.org), previously characterized metagenomically derived GH94s[39] and GH94 sequences found in the *A. laidlawii* genome[40] (Figure 1). AchP was found to be one of 23 singletons that do not share a pairwise sequence identity of over 40% with any other GH94 sequence. The member that shared AchP's lowest *E*-value of 1.1×10^{-175}, with a pairwise score of 37%, is marked with a black arrow in Figure 1 and resides as a doublet in cluster 94-17. The member that shared the lowest *E*-value (9.5×10^{-27}), which also belonged to a cluster containing functionally characterized members, is located in 94-1B. However, the *E*-value between these two sequences fell well short of the threshold and therefore provided no information toward determining AchP's activity. Given that SSN analysis failed to cluster AchP with any characterized GH94 that may suggest its activity but instead classified it as a singleton, we considered the possibility that AchP may represent a new activity within the GH94 family.

Substrate Specificity Screen. AchP was heterologously expressed, purified, and screened in the absence of cell lysate against an extended set of donors and acceptors, including additional *N*-acetamido sugars. To do this, we used a phosphorylase screening method described previously that couples the chromogenic development of molybdenum blue to the liberation of free phosphate during reverse phosphorolysis[39,41] (Figure 2A). When incubated with Glc1-P as a donor, AchP was active in the presence of acceptors GlcNAc, GlcNAc-β-pNP, GalNAc, and GlcNAc-β1,4-GlcNAc, while no activity was detected with the nonacetylated glucosamine and galactosamine. With GlcNAc1-P as a donor, AchP was active with all acceptors that contained an *N*-acetyl moiety as well as with glucose and glucosamine but not galactose and galactosamine. Lastly, when GalNAc1-P was used as a donor, the activity could only be detected when GlcNAc was the acceptor. These results show that GlcNAc1-P is a superior donor relative to Glc1-P and, thus, that the binding of an acetamide in the −1 (donor) subsite is advantageous. Of the 11 acceptors screened, only GlcNAc was able to stimulate activity in the presence of every donor assayed, indicating that, again, an equatorial acetamide moiety is preferred on the sugar that binds in the +1 subsite. Interestingly, however, GalNAc, with an axial C4 hydroxyl, also proved to be a good acceptor, as does an axial glycoside thereof.

To quantitate this specificity, kinetic parameters were determined for reaction with the acceptors, GlcNAc or GalNAc, each in the presence of fixed concentrations of either donor, Glc1-P or GlcNAc1-P (Table 1 and Figure S2). Activities were too low with the donor GalNAc1-P or the acceptor glucose when using reasonable substrate and enzyme concentrations, so kinetic parameters were not determined in that case. GlcNAc1-P is the preferred donor over Glc1-P, with a corresponding K_m value (GlcNAc) almost 10-fold lower and k_{cat} 2-fold greater, confirming and quantitating the importance of the equatorial C-2 acetamide. The very low activity with GalNAc1-P shows that an axial hydroxyl at C-4 is not well-accommodated at the donor site, though GalNAc binds well in the acceptor locus.

Of the seven activities described to date in the GH94 family, only the *N*,*N*′-diacetylchitobiose phosphorylases (ChbP) are known to use GlcNAc1-P as a donor, transferring only to monosaccharide GlcNAc acceptors and not to di- or trisaccharides. The six other types types utilize Glc1-P. The bacteria from which both characterized ChbPs were discovered are native to marine environments where chitin, a polysaccharide of β1,4-linked GlcNAc and the primary structural component of the exoskeleton of marine invertebrates, is common. These ChbPs presumably act on disaccharides released from chitin by chitinases. AchP on the other hand is able to utilize GlcNAc-β1,4-GlcNAc and GlcNAc(-β1,4-GlcNAc)$_3$ as acceptors performing iterative addition of *N*-

https://doi.org/10.1021/acscentsci.1c01570
ACS Cent. Sci. XXXX, XXX, XXX−XXX

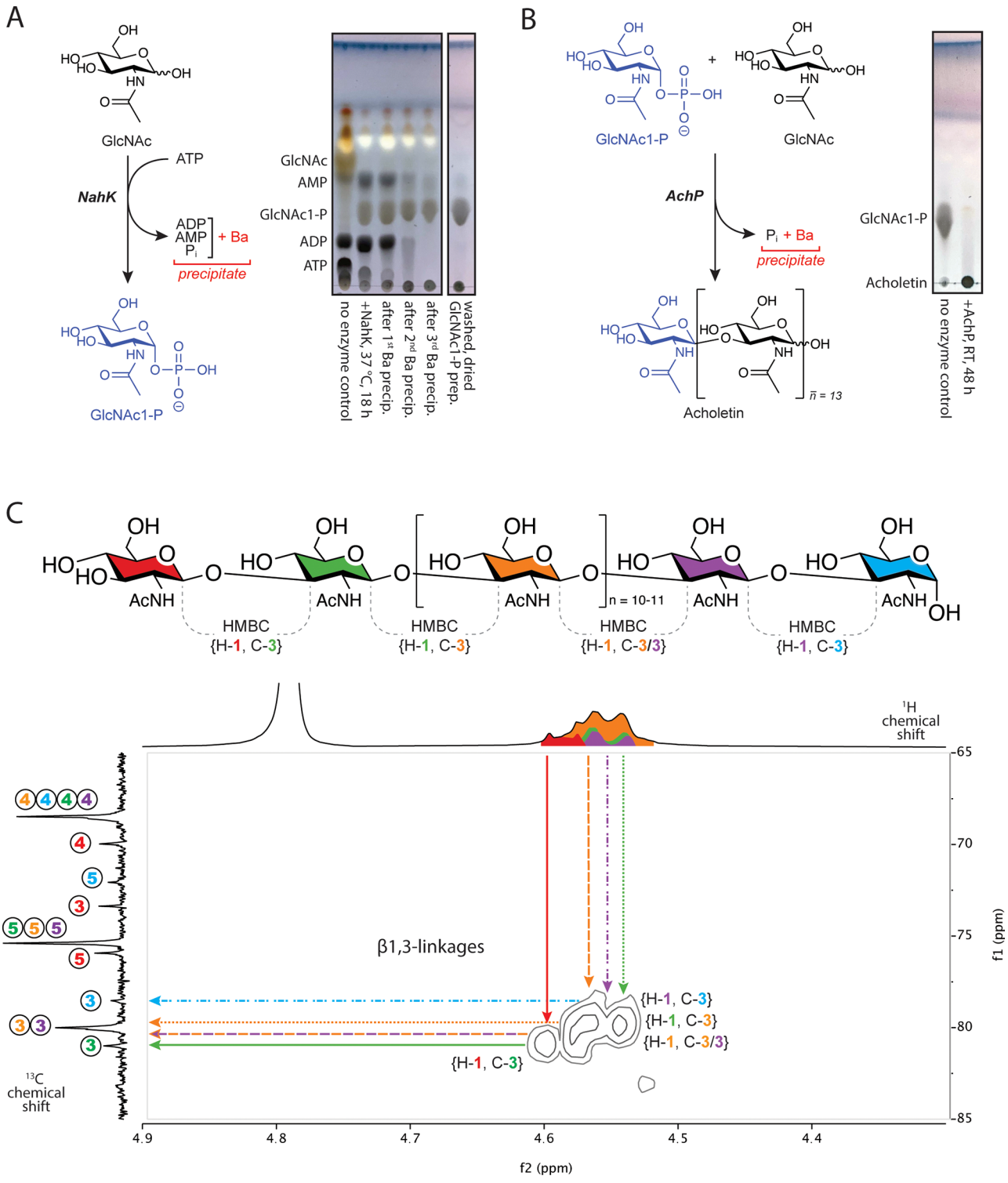

Figure 3. Two-pot large-scale acholetin synthesis. (A) Pot one. NahK-catalyzed production of GlcNAc1-P. Sequential barium precipitation was performed to reduce ADP, AMP, and inorganic phosphate concentrations following the completion of the reaction. GlcNAc1-P preparation was precipitated with ethanol and then dried. (B) Pot two. AchP-catalyzed production of acholetin. Following the completion of the reaction, the acholetin sample was desalted with G25 resin (Figure S7) prior to lyophilization and product analysis. (C) Acholetin HMBC NMR analysis. Overlapping correlations were resolved with the help of ^{1}H, ^{13}C, COSY, and HSQC experiments (^{13}C shown in Figure S8).

acetylglucosaminyl residues (Figure S3A). As noted earlier, we initially anticipated that AchP was a chitin phosphorylase. However, when we assayed for phosphorolysis of GlcNAc-β1,4-GlcNAc, no substrate cleavage could be detected (Figure S3B). Although a surprising result at the time, it perhaps should not have been given the previous results showing that AchP transfers to GalNAc, which has an inverted stereochemistry at C-4 relative to GlcNAc. Such transfer would not be expected if the enzyme were 1,4-specific since the hydroxyl at C-4 would be incorrectly oriented (Figure S4). These results led us to suspect that a different linkage was being formed/broken by AchP.

https://doi.org/10.1021/acscentsci.1c01570
ACS Cent. Sci. XXXX, XXX, XXX−XXX

Linkage Determination. The two other potential linkages that AchP could be creating are β1,3 or β1,6, and so a product analysis was necessary. Two AchP product glycans were thus analyzed by NMR spectroscopy. The first was the GlcNAc−GlcNAc disaccharide product formed when GlcNAc1-P and GlcNAc were used as the donor/acceptor combination. A β1,3 glycosidic linkage was detected from a heteronuclear multiple bond correlation (HMBC) experiment (Figure S5). A through-bond correlation was detected between the nonreducing end anomeric proton and the C-3 carbon (in α and β anomeric configuration, both of which are shifted ∼7 ppm downfield as compared to unlinked GlcNAc) of the reducing end GlcNAc. In order to confirm that use of a different donor does not change the linkage formed, we also analyzed the Glc-GlcNAc-α-pNP produced with Glc1-P as the donor and the aryl glycoside GlcNAc-α-pNP as the acceptor. The C-4 and C-6 chemical shifts (68.22 and 60.37, respectively) remained approximately equivalent compared to free GlcNAc, whereas the C-3 (82.03) signal was shifted downfield, consistent with the 1,3 linkage. Therefore, through NMR analysis, it was confirmed that AchP generates β1,3 glycosidic linkages when either GlcNAc1-P or Glc1-P was used as the donor, as shown in Figure 2B, when using GlcNAc residues as the donor and acceptor.

Formation of Polymeric Products. In general, glycoside phosphorylases either show a specificity for disaccharides or prefer polymeric substrates, with the GH149 β-1,3-oligoglucan phosphorylases being exceptions in that they display both di- and oligosaccharide phosphorylase activities.[39,42] AchP also appears to possess both activities since it can use both the monosaccharide GlcNAc and the disaccharide *N*,*N*′-diacetylchitobiose as acceptors, with TLC analysis confirming the elongation of each acceptor (GlcNAc, GlcNAc-β1,4-GlcNAc, and GlcNAc(-β1,4-GlcNAc)$_3$ with the donor GlcNAc1-P; Figure S3A).

To study the oligomerization further, the degree of polymerization (DP) of the product glycans in the presence of varying concentrations of different donors and acceptors was determined (Figure 2C and Figure S6). Reactions were carried out in the presence of 10 mM donor and either 100, 10, or 0.1 mM GlcNAc, giving donor-to-acceptor ratios of 1:10, 1:1, and 100:1, respectively. When GlcNAc1-P was used as the donor, the maximum DPs detected by MALDI-MS were 3, 6, and 13 with donor-to-acceptor ratios of 1:10, 1:1, and 100:1, respectively. When GalNAc1-P was the donor, the maximum DPs were 3, 4, and 6, respectively (Figure 2C). Similar reactions in which GalNAc replaced GlcNAc as the acceptor (Figure S6) resulted in the same general pattern of oligomerization. However, when Glc1-P was used at donor-to-acceptor ratios of 1:10 and 1:1, no products with a DP greater than 2 could be detected, indicating that the product Glc-β1,3-GlcNAc does not act as an acceptor when Glc1-P is the donor. This is consistent with the substrate specificity results described above (Figure 2A) where no activity could be observed with the donor Glc1-P and acceptors glucose or laminaribiose (Glc-β1,3-Glc), further highlighting the importance of a C-2 acetamide in the +1 subsite. Therefore, like the GH149 β-1,3-oligoglucan phosphorylases, AchP also acts as a dual di- and oligosaccharide phosphorylase with the donors GlcNAc1-P or GalNAc1-P, but when Glc1-P is the donor, AchP acts as a strict disaccharide phosphorylase.

Two-Pot Large-Scale Acholetin Synthesis. To demonstrate the scalability of the reaction, acholetin synthesis was coupled to GlcNAc1-P production with the aid of an *N*-acetylhexosamine-1-kinase from *Bifidobacterium longum* JCM1217 (NahK)[43] in a two-pot reaction scheme (Figure 3A,B). In the first pot, GlcNAc was combined with ATP (molar ratio of 1 GlcNAc to 1.3 ATP) and incubated with NahK for 18 h at 37 °C (Figure 3A). Sequential barium acetate precipitations removed ADP, AMP, free phosphate, as well as any unreacted ATP. After the final barium precipitation, GlcNAc1-P, along with some barium acetate, was precipitated with ethanol and then washed with acetone before being dried under vacuum. The barium salt was not purified away since it helps by precipitating phosphate liberated during the subsequent AchP reaction, driving the reaction toward synthesis. In the second pot, the GlcNAc1-P preparation was dissolved in buffer containing AchP and GlcNAc at a donor/acceptor ratio of ∼1000:1 and incubated at room temperature for 48 h, at which point no more GlcNAc1-P could be detected by TLC (Figure 3B). After removing the precipitated barium phosphate salt and enzyme by heating and centrifugation, the reaction mixture was desalted to remove the remaining soluble barium acetate (Figure S7) and then lyophilized to produce a white, fluffy material. The recovered product mass was 344.3 mg from 1 g of GlcNAc.

Multiangle light scattering analysis on the purified acholetin yielded an average molecular weight of 2966 ± 22 g/mol, indicating an average DP of 14.6 GlcNAc residues per acholetin molecule while the structure was confirmed by NMR spectroscopy (HMBC). Multiple through-bond correlations corresponding to pairs between H-1 and C-3 from the adjacent unit established the "HMBC" marked linkages shown on the acholetin structure in Figure 3C. The presence of both α- and β-anomers at the reducing end and the multiple GlcNAc units made the assignment of chemical shifts a challenge. Therefore, the same acholetin sample was reduced with sodium borohydride, and the resultant ^{13}C NMR spectrum was compared to that of the parent sugar to identify resonances from the reducing end unit and to correctly assign the corresponding chemical shifts (Figure S8). Only β1,3 linkages were found.

Further confirmation of the linkage type was obtained through enzymatic digestion studies. The treatment of acholetin either with an endochitinase from *Streptomyces griseus* (sgChit), which hydrolytically cleaves β1,4 linkages, or with dispersin B (dspB),[44] which cleaves β1,6 linkages, resulted in no degradation (Figure S9). By contrast, sgChit and dspB were shown to degrade chito-oligosaccharides and PNAG, respectively, but not acholetin, as would be expected (Figure S9, middle and bottom). However, Acholetin was degraded, as also were chitin and PNAG oligos, by an exolytic β-*N*-acetylhexosaminidase from *Streptomyces plicatus* (spHex) (Figure S9, top), which progressively cleaves nonreducing end GlcNAc residues from a range of glycoconjugates and oligo- and polysaccharides.[45−47]

These studies confirm the structure of this new GlcNAc-based homopolymer, acholetin, which has considerable potential as a new biomaterial. Inexpensive production of this polymer should be feasible by generation of the GlcNAc1-P donor through phosphorylase-catalyzed degradation of chitin, possibly in a reaction coupled with a suitable chitinase.

Core 3 Mucin-Type *O*-Glycan Analogue. The ability of this enzyme to efficiently transfer GlcNAc to GalNAc with a 1,3 linkage opens the possibility of using this enzyme to make core 3 mucin-type *O*-glycan structures (GlcNAc-β1,3-GalNAc-α-OR). Enzymatic syntheses of these structures are generally challenging due to the instability of the β1,3-GlcNAc transferase responsible for its synthesis *in vivo*.[48] Using AchP, two core 3

https://doi.org/10.1021/acscentsci.1c01570
ACS Cent. Sci. XXXX, XXX, XXX−XXX

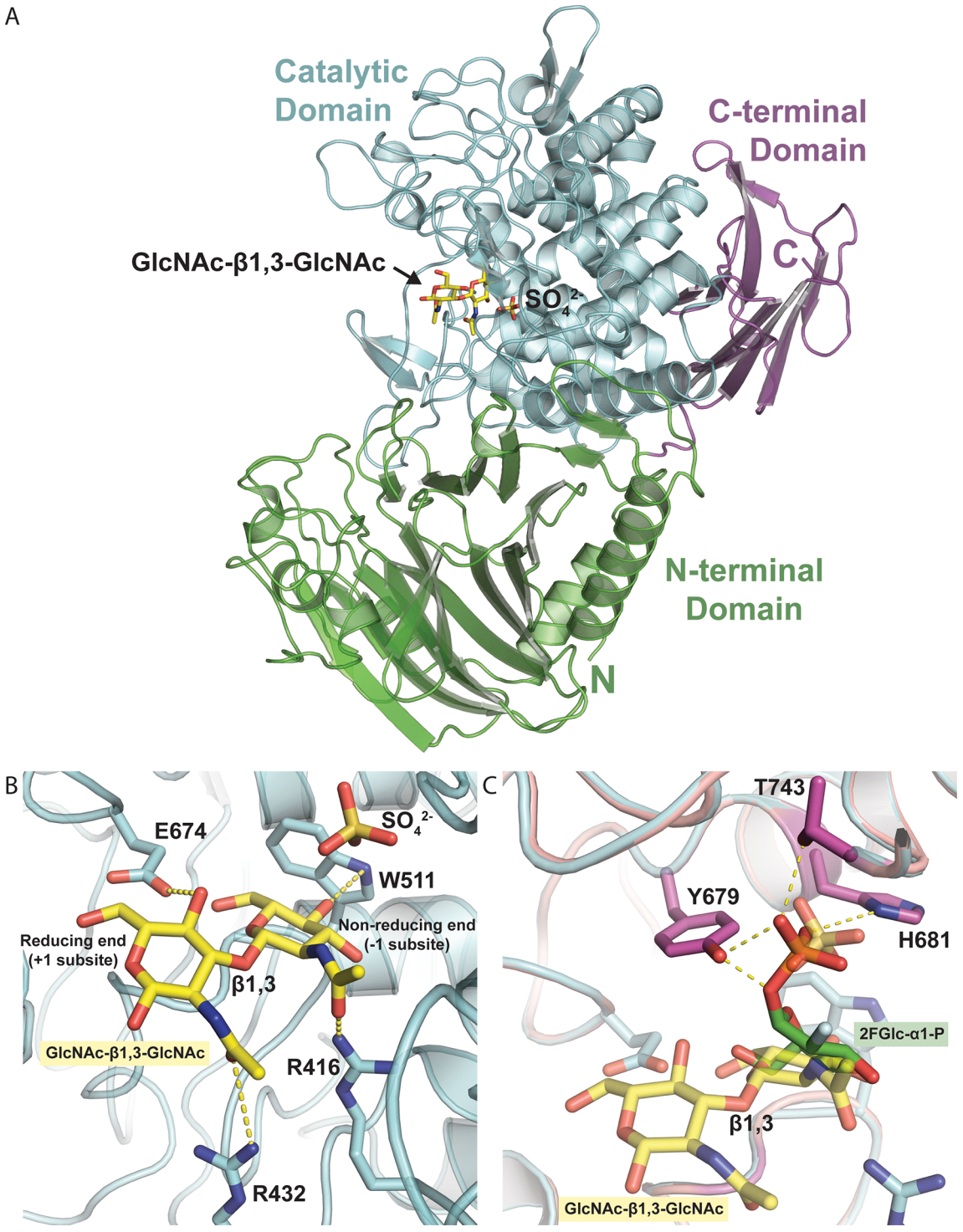

Figure 4. Crystal structure of AchP and the GlcNAc-β1,3-GlcNAc complex. (A) Cartoon representation of the D513A-AchP structure in complex with GlcNAc-β1,3-GlcNAc and SO_4^{2-} in the active site. (B) Zoomed view of the active site showing the +1 reducing end and −1 nonreducing end of the GlcNAc-β1,3-GlcNAc substrate. Side chain residues R416, R432, W511, and E674 that form hydrogen bonds represented by yellow dashed lines; SO_4 bound to the phosphate binding site. (C) A superposition of the D513A-AchP/GlcNAc-β1,3-GlcNAc (cyan) and wild-type AchP/2FGlc-α1-P (pink) structures shows the phosphate group of 2FGlc-α1-P H-bonds with the residues Y679 and T743 (represented by a yellow dashed line).

analogues were made using GlcNAc1-P as the donor and either 4-methylumbelliferyl *N*-acetyl-α-D-galactosaminide (GalNAc-α-MU) or GalNAc-α-pNP as acceptors to generate GlcNAc-β1,3-GalNAc-α-MU (Figure S10A) and GlcNAc-β1,3-GalNAc-α-pNP (Figure S10B), as confirmed by TLC and mass spectrometry. Further confirmation of product identity was obtained by treatment with a GH101 endo-α-*N*-acetylgalactosaminidase from *Streptococcus pneumoniae* (EngSP), which is known to cleave the disaccharide moiety from GlcNAc-β1,3-GalNAc-α1-pNP, releasing pNP.[49] After incubation with EngSP, a release of both pNP and MU aglycones could be detected (Figure S10C,D), with only minimal aglycone release in controls.

https://doi.org/10.1021/acscentsci.1c01570
ACS Cent. Sci. XXXX, XXX, XXX−XXX

Crystallographic Determination of the AchP Structure. The crystal structure of wild-type AchP was determined by single wavelength anomalous diffraction (SAD) experimental phasing using a Se-Met-labeled protein since the closest homologue structure deposited at PDB[50] showed only 23% identity. The overall fold of AchP (residues 1−842) can be best described as a 3 domain architecture. The N-terminal domain (residues 1−330) is composed of antiparallel β-strands forming two β-sheets facing each other, a catalytic domain (residues 344−759) with an $(\alpha/\alpha)_6$-barrel fold, and a C-terminal β-sandwich domain (residues 331−343 and residues 760−842) (Figure 4A). The oligomeric state of AchP proved to be a dimer where the N-terminal domain residues from interacting monomers contribute to active site formation (Figure S11).

To gain structural insights into its substrate specificity and mechanism, a mutant was generated through alanine substitution of the catalytic acid/base residue, D513, which rendered the enzyme catalytically inactive (Figures S12 and S13). D513 is equivalent to residues assigned as the critical acid/base residue in other GH94 enzymes.[51] Crystals of the D513A-AchP mutant were then soaked with the GlcNAc-β1,3-GlcNAc ligand. The structure of D513A-AchP clearly showed GlcNAc-β1,3-GlcNAc bound in the active site, with a sulfate group located at the putative phosphate binding site (Figure 4B and Figure S14). Given their common tetrahedral geometry, it was reassuring to capture the catalytically inactive sulfate in the active site appropriately positioned to perform nucleophilic attack on the anomeric carbon of the nonreducing end residue. This therefore likely represents the true phosphate binding site for the reaction in the direction of phosphorolysis. To gain insight into the binding mode for reaction in the reverse direction—glycoside synthesis—we took advantage of the fact that this enzyme catalyzes the transfer from Glc-α1-P as well as GlcNAc1-P, and we used 2FGlc-α1-P as an enzymatically inert substrate analogue.[52] The crystal structure of wild-type AchP in complex with the inactive donor substrate analogue 2FGlc-α1-P revealed the substrate bound with the sugar ring in a boat/skew boat conformation. An overlay of the two structures (Figure 4C) revealed that the phosphate moiety of 2FGlc-α1-P and the sulfate bound in essentially the same position in the active site with the phosphate moiety held in position through polar interactions with residues H681, Y679, and T743, highlighting their importance for phosphate binding.

The structural basis for the requirement for an acetamido group at C2 of each of the sugar residues is revealed in the binding mode of GlcNAc-β1,3-GlcNAc where the nonreducing end NAc group interacts with R416 and the reducing end NAc group interacts with R432. Similar interactions would not be feasible with a hydroxyl at those positions. The previously observed preference for GlcNAc acceptors over GalNAc is similarly explained through the polar interaction of the 4-hydroxyl of the nonreducing end GlcNAc residue with W511 and the reducing end 4-hydroxyl with E674. These interactions would be completely missing for GalNAc, where the hydroxyl group is in an axial orientation at C-4 (Figure 4B). The preference of AchP for GlcNAc1-P as the donor over GalNAc1-P is likewise probably due to the polar interaction formed between the equatorial hydroxyl at C4 of the donor sugar and W511 (Figure 4B).

The structural overlay in Figure 4C also nicely illustrates the reaction mechanism wherein binding of the sugar-1-phosphate in a boat/skew boat conformation enforces partial planarity on the sugar ring around the anomeric center as required for oxocarbenium ion formation at the transition state. Reaction occurs through electrophilic migration of the anomeric center from the phosphate oxygen onto the 3-hydroxyl of the acceptor sugar with base catalytic assistance from D513. In the process, the transferred sugar ring relaxes back to its $^4C_1$ conformation in the disaccharide product, which then diffuses from the active site. This is the same conformational itinerary seen for inverting β-glucosidases from the glycoside hydrolase CAZy family GH8.[53,54]

AchP and Acholetin's Biological Role. *A. laidlawii* was first identified in 1936 from raw London (England) sewage by Laidlaw and Elford.[55] The organism is a common mycoplasma widely found throughout nature, including in human, animal, and plant tissues.[56,57] It is also a predominant contaminant of cell cultures, which presents significant concerns for a range of biotechnology sectors.[56,58,59] Mycoplasma are one of the smallest living forms of microbes and notably differ from other bacteria because they lack a cell wall.[60] Research performed on the organism in the first half of the 1970s suggested that a high-molecular-weight polysaccharide was weakly associated with the exterior surface of the plasma membrane.[61,62] This could help stabilize the organism and is thought to be the major antigenic determinant of *A. laidlawii* membranes.[63] Furthermore, this polysaccharide was shown to contain exclusively GlcNAc and GalNAc residues;[61,63] however, to our knowledge, the exact chemical structure (including glycosidic linkage type) and functional role of this polyhexosamine have never been determined. We hypothesize that AchP is involved with the maintenance, in a biodegradative role, of this membrane associated polyhexosamine.

Summary. Through the phylogenomic exploration of the GH94 family, we have discovered the novel biopolymer acholetin that has wide ranging potential as a new type of biocompatible and biodegradable material, or component thereof. Further, we have developed an efficient method to enzymatically synthesize acholetin utilizing the reverse phosphorolysis action of the novel acholetin phosphorylase, identified within the genome of the cell-wall-less mycoplasma bacterium *Acholeplasma laidlawii*. It is not yet understood how *A. laidlawii* biosynthesizes acholetin, but perhaps the yet unclassified glycosyltransferase (GT) (ABX81652) found in proximity to the AchP coding region in the *A. laidlawii* genome may be implicated. Despite significant effort, we were not able to test this possibility because we were unable to express this unclassified GT in a soluble active form. Many GTs that act on secreted bacterial polysaccharides are membrane-bound enzymes and therefore can be challenging to express.[64] Nevertheless, we have likely uncovered the identity of the high-molecular-weight biopolymer associated with the *A. laidlawii* membrane discovered almost five decades ago. With this knowledge, new strategies can begin to be developed aiming to degrade or disrupt the formation of acholetin. These strategies could then be deployed either in a biotechnology context to destabilize the *A. laidlawii* membrane, thereby preventing or limiting cell culture contamination, or in a medical context, by eliminating what is thought to be *A. laidlawii*'s major antigenic determinant.

■ ASSOCIATED CONTENT

Supporting Information

The Supporting Information is available free of charge at https://pubs.acs.org/doi/10.1021/acscentsci.1c01570.

https://doi.org/10.1021/acscentsci.1c01570
ACS Cent. Sci. XXXX, XXX, XXX−XXX

Experimental methods and additional data and figures including a specificity screen, Michaelis−Menten plots, TLC results, reaction mechanisms, HMBC results, DP analysis, NMR results, degradation assay, structures, and electron density maps (PDF)

AUTHOR INFORMATION

Corresponding Author

Stephen G. Withers − *Michael Smith Laboratories, University of British Columbia, Vancouver, British Columbia V6T 1Z4, Canada; Department of Chemistry, University of British Columbia, Vancouver, British Columbia V6T 1Z1, Canada; Department of Biochemistry & Molecular Biology, University of British Columbia, Vancouver, British Columbia V6T 1Z4, Canada;* orcid.org/0000-0002-6722-5701; Email: withers@chem.ubc.ca

Authors

Spencer S. Macdonald − *Michael Smith Laboratories, University of British Columbia, Vancouver, British Columbia V6T 1Z4, Canada; Department of Chemistry, University of British Columbia, Vancouver, British Columbia V6T 1Z1, Canada*

Jose H. Pereira − *Joint BioEnergy Institute, Emeryville, California 94608, United States; Molecular Biophysics & Integrated Bioimaging Division, Lawrence Berkeley National Laboratory, Berkeley, California 94720, United States*

Feng Liu − *Department of Chemistry, University of British Columbia, Vancouver, British Columbia V6T 1Z1, Canada*

Gregor Tegl − *Department of Chemistry, University of British Columbia, Vancouver, British Columbia V6T 1Z1, Canada*

Andy DeGiovanni − *Joint BioEnergy Institute, Emeryville, California 94608, United States; Molecular Biophysics & Integrated Bioimaging Division, Lawrence Berkeley National Laboratory, Berkeley, California 94720, United States*

Jacob F. Wardman − *Michael Smith Laboratories, University of British Columbia, Vancouver, British Columbia V6T 1Z4, Canada; Department of Biochemistry & Molecular Biology, University of British Columbia, Vancouver, British Columbia V6T 1Z4, Canada;* orcid.org/0000-0002-8235-3576

Samuel Deutsch − *The US Department of Energy Joint Genome Institute, Lawrence Berkley National Laboratory, Berkeley, California 94720, United States*

Yasuo Yoshikuni − *The US Department of Energy Joint Genome Institute, Lawrence Berkley National Laboratory, Berkeley, California 94720, United States;* orcid.org/0000-0002-8372-640X

Paul D. Adams − *Joint BioEnergy Institute, Emeryville, California 94608, United States; Molecular Biophysics & Integrated Bioimaging Division, Lawrence Berkeley National Laboratory, Berkeley, California 94720, United States; Department of Bioengineering, University of California Berkeley, Berkeley, California 94720, United States*

Complete contact information is available at: https://pubs.acs.org/10.1021/acscentsci.1c01570

Author Contributions

Conceptualization: S.S.M., S.D., Y.Y., and S.G.W. Methodology: S.S.M., J.H.P., F.L., G.T., and J.F.W. Software: S.S.M. Validation: S.S.M., J.H.P., F.L., and G.T. Formal Analysis: S.S.M., J.H.P., F.L., and G.T. Investigation: S.S.M., J.H.P., F.L., G.T., A.D., and S.D. Data curation: S.S.M., J.H.P., F.L., and G.T. Writing—original draft: S.S.M. Writing—review and editing: S.S.M., J.H.P., and S.G.W. Visualization: S.S.M., J.H.P., and F.L. Supervision: Y.Y., P.D.A., and S.G.W. Funding Acquisition: Y.Y., P.D.A., and S.G.W.

Notes

The authors declare no competing financial interest.

ACKNOWLEDGMENTS

We thank Dr. Hongming Chen for reagents and Dr. Mark Nitz (U of Toronto) for a generous donation of dispersin B and PNG oligosaccharides. We also thank Dr. Jayachandran Kizhakkedathu for access to the multiangle light scattering instrument and Irina Chafeeva for the technical assistance. We thank the Natural Sciences and Engineering Research Council of Canada (NSERC) and the Canadian Institutes for Health Research (CIHR) for financial support of this work. The work conducted by the US Department of Energy Joint Genome Institute, a DOE Office of Science User Facility, is supported by the Office of Science of the US Department of Energy under Contract DE-AC02-05CH11231. The work conducted by the Joint BioEnergy Institute is supported by the US Department of Energy, Office of Science, Office of Biological and Environmental Research under Contract DE-AC02-05CH11231 between LBNL and the US Department of Energy. The Advanced Light Source is a Department of Energy Office of Science User Facility under Contract DE-AC02-05CH11231. The Berkeley Center for Structural Biology is supported in part by the Howard Hughes Medical Institute. The ALS-ENABLE beamlines are supported in part by the National Institutes of Health, National Institute of General Medical Sciences, Grant P30 GM124169.

ABBREVIATIONS

GP, glycoside phosphorylase; CAZy, carbohydrate active enzyme; AchP, acholetin phosphorylase; NahK, *N*-acetylhexosamine-1-kinase; EngSP, endo-α-*N*-acetylgalactosamindase; spHex, β-*N*-acetylhexosaminidase; dspB, dispersin B; sgChit, endochitinase; Glc, glucose; Gal, galactose; GlcN, glucosamine; GalN, galactosamine; ManNAc, *N*-acetylmannosamine; GlcNAc, *N*-acetylglucosamine; GalNAc, *N*-acetylgalactosamine; PNAG, poly-β-1,6-*N*-acetylglucosamine; Glc1-P, α-glucose 1-phosphate; GlcNAc1-P, α-*N*-acetylglucosamine 1-phosphate; GalNAc1-P, α-*N*-acetylgalactosamine 1-phosphate; MU, 4-methylumbelliferyl; pNP, 4-nitrophenol; ATP, adenosine triphosphate; ADP, adenosine diphosphate; AMP, adenosine monophosphate; SSN, sequence similarity network; CAZy DB, Carbohydrate Active Enzymes database; PDB, Protein Data Bank; ChbP, *N*,*N*′-diacetylchitobiose phosphorylase; NMR, nuclear magnetic resonance; HMBC, heteronuclear multiple bond correlation; TLC, thin layer chromatography; DP, degree of polymerization

REFERENCES

(1) Song, E.-H.; Shang, J.; Ratner, D. M. Polysaccharides. In *Polymer Science: A Comprehensive Reference*; Elsevier, 2012; Vol. 9, pp 137−155.

(2) Smith, P. J.; Ortiz-Soto, M. E.; Roth, C.; Barnes, W. J.; Seibel, J.; Urbanowicz, B. R.; Pfrengle, F. Enzymatic Synthesis of Artificial Polysaccharides. *ACS Sustainable Chem. Eng.* **2020**, *8* (32), 11853−11871.

(3) Seeberger, P. H.; Werz, D. B. Synthesis and Medical Applications of Oligosaccharides. *Nature* **2007**, *446* (7139), 1046−1051.

https://doi.org/10.1021/acscentsci.1c01570
ACS Cent. Sci. XXXX, XXX, XXX−XXX

(4) Yu, Y.; Shen, M.; Song, Q.; Xie, J. Biological Activities and Pharmaceutical Applications of Polysaccharide from Natural Resources: A Review. *Carbohydr. Polym.* **2018**, *183*, 91−101.
(5) Felt, O.; Buri, P.; Gurny, R. Chitosan: A Unique Polysaccharide for Drug Delivery. *Drug Dev. Ind. Pharm.* **1998**, *24* (11), 979−993.
(6) Zhang, N.; Wardwell, P. R.; Bader, R. A. Polysaccharide-Based Micelles for Drug Delivery. *Pharmaceutics* **2013**, *5* (2), 329−352.
(7) Debele, T. A.; Mekuria, S. L.; Tsai, H. C. Polysaccharide Based Nanogels in the Drug Delivery System: Application as the Carrier of Pharmaceutical Agents. *Materials Science and Engineering C* **2016**, *68*, 964−981.
(8) Sinha, V. R.; Kumria, R. Polysaccharides in Colon-Specific Drug Delivery. *Int. J. Pharm.* **2001**, *224* (1−2), 19−38.
(9) Liu, Z.; Jiao, Y.; Wang, Y.; Zhou, C.; Zhang, Z. Polysaccharides-Based Nanoparticles as Drug Delivery Systems. *Adv. Drug Delivery Rev.* **2008**, *60* (15), 1650−1662.
(10) Barclay, T. G.; Day, C. M.; Petrovsky, N.; Garg, S. Review of Polysaccharide Particle-Based Functional Drug Delivery. *Carbohydr. Polym.* **2019**, *221*, 94−112.
(11) Saidin, N. M.; Anuar, N. K.; Meor Mohd Affandi, M. M. R. Roles of Polysaccharides in Transdermal Drug Delivery System and Future Prospects. *Journal of Applied Pharmaceutical Science* **2018**, *8* (3), 141−157.
(12) Hudak, J. E.; Bertozzi, C. R. Glycotherapy: New Advances Inspire a Reemergence of Glycans in Medicine. *Chemistry and Biology* **2014**, *21* (1), 16−37.
(13) Yu, X.; Marshall, M. J. E.; Cragg, M. S.; Crispin, M. Improving Antibody-Based Cancer Therapeutics Through Glycan Engineering. *BioDrugs* **2017**, *31* (3), 151−166.
(14) Yang, X.; Bartlett, M. G. Glycan Analysis for Protein Therapeutics. *Journal of Chromatography B: Analytical Technologies in the Biomedical and Life Sciences* **2019**, *1120*, 29−40.
(15) Zahedi, P.; Rezaeian, I.; Ranaei-Siadat, S.-O.; Jafari, S.-H.; Supaphol, P. A Review on Wound Dressings with an Emphasis on Electrospun Nanofibrous Polymeric Bandages. *Polym. Adv. Technol.* **2010**, *21* (2), 77−95.
(16) Fürsatz, M.; Skog, M.; Sivlér, P.; Palm, E.; Aronsson, C.; Skallberg, A.; Greczynski, G.; Khalaf, H.; Bengtsson, T.; Aili, D. Functionalization of Bacterial Cellulose Wound Dressings with the Antimicrobial Peptide Epsilon-Poly-L-Lysine. *Biomedical Materials (Bristol)* **2018**, *13* (2), 025014.
(17) Aduba, D. C.; Yang, H. Polysaccharide Fabrication Platforms and Biocompatibility Assessment as Candidate Wound Dressing Materials. *Bioengineering* **2017**, *4* (1), 1.
(18) Wittaya-Areekul, S.; Prahsarn, C. Development and in Vitro Evaluation of Chitosan-Poly-Saccharides Composite Wound Dressings. *Int. J. Pharm.* **2006**, *313* (1−2), 123−128.
(19) Naseri-Nosar, M.; Ziora, Z. M. Wound Dressings from Naturally-Occurring Polymers: A Review on Homopolysaccharide-Based Composites. *Carbohydr. Polym.* **2018**, *189*, 379−398.
(20) Zhang, Y. S.; Yue, K.; Aleman, J.; Mollazadeh-Moghaddam, K.; Bakht, S. M.; Yang, J.; Jia, W.; Dell'Erba, V.; Assawes, P.; Shin, S. R.; et al. 3D Bioprinting for Tissue and Organ Fabrication. *Annals of Biomedical Engineering* **2017**, *45* (1), 148−163.
(21) Shin, J. Y.; Yeo, Y. H.; Jeong, J. E.; Park, S. A.; Park, W. H. Dual-Crosslinked Methylcellulose Hydrogels for 3D Bioprinting Applications. *Carbohydr. Polym.* **2020**, *238*, 116192.
(22) Zennifer, A.; Senthilvelan, P.; Sethuraman, S.; Sundaramurthi, D. Key Advances of Carboxymethyl Cellulose in Tissue Engineering & 3D Bioprinting Applications. *Carbohydr. Polym.* **2021**, *256*, 117561.
(23) Li, S.; Tian, X.; Fan, J.; Tong, H.; Ao, Q.; Wang, X. Chitosans for Tissue Repair and Organ Three-Dimensional (3D) Bioprinting. *Micromachines* **2019**, *10* (11), 765.
(24) Xu, J.; Zheng, S.; Hu, X.; Li, L.; Li, W.; Parungao, R.; Wang, Y.; Nie, Y.; Liu, T.; Song, K. Advances in the Research of Bioinks Based on Natural Collagen, Polysaccharide and Their Derivatives for Skin 3D Bioprinting. *Polymers* **2020**, *12* (6), 1237.
(25) McCarthy, R. R.; Ullah, M. W.; Booth, P.; Pei, E.; Yang, G. The Use of Bacterial Polysaccharides in Bioprinting. *Biotechnology Advances* **2019**, *37* (8), 107448.
(26) Mohan, T.; Maver, T.; Štiglic, A. D.; Stana-Kleinschek, K.; Kargl, R. 3D Bioprinting of Polysaccharides and Their Derivatives: From Characterization to Application. In *Fundamental Biomaterials: Polymers*; Elsevier, 2018; pp 105−141.
(27) Xiao, R.; Grinstaff, M. W. Chemical Synthesis of Polysaccharides and Polysaccharide Mimetics. *Prog. Polym. Sci.* **2017**, *74*, 78−116.
(28) Danby, P. M.; Withers, S. G. Advances in Enzymatic Glycoside Synthesis. *ACS Chem. Biol.* **2016**, *11* (7), 1784−1794.
(29) Kadokawa, J. I. Precision Polysaccharide Synthesis Catalyzed by Enzymes. *Chem. Rev.* **2011**, *111* (7), 4308−4345.
(30) Lombard, V.; Golaconda Ramulu, H.; Drula, E.; Coutinho, P. M.; Henrissat, B. The Carbohydrate-Active Enzymes Database (CAZy) in 2013. *Nucleic Acids Res.* **2014**, *42* (D1), D490−D495.
(31) Nakai, H.; Kitaoka, M.; Svensson, B.; Ohtsubo, K. Recent Development of Phosphorylases Possessing Large Potential for Oligosaccharide Synthesis. *Curr. Opin. Chem. Biol.* **2013**, *17* (2), 301−309.
(32) O'Neill, E. C.; Field, R. A. Enzymatic Synthesis Using Glycoside Phosphorylases. *Carbohydr. Res.* **2015**, *403*, 23−37.
(33) Puchart, V. Glycoside Phosphorylases: Structure, Catalytic Properties and Biotechnological Potential. *Biotechnology Advances* **2015**, *33* (2), 261−276.
(34) Awad, F. N. Glycoside Phosphorylases for Carbohydrate Synthesis: An Insight into the Diversity and Potentiality. *Biocatalysis and Agricultural Biotechnology* **2021**, *31*, 101886.
(35) Zallot, R.; Oberg, N.; Gerlt, J. A. The EFI Web Resource for Genomic Enzymology Tools: Leveraging Protein, Genome, and Metagenome Databases to Discover Novel Enzymes and Metabolic Pathways. *Biochemistry* **2019**, *58* (41), 4169−4182.
(36) Zallot, R.; Oberg, N. O.; Gerlt, J. A. 'Democratized' Genomic Enzymology Web Tools for Functional Assignment. *Curr. Opin. Chem. Biol.* **2018**, *47*, 77−85.
(37) Gerlt, J. A. Genomic Enzymology: Web Tools for Leveraging Protein Family Sequence-Function Space and Genome Context to Discover Novel Functions. *Biochemistry* **2017**, *56* (33), 4293−4308.
(38) Gerlt, J. A.; Bouvier, J. T.; Davidson, D. B.; Imker, H. J.; Sadkhin, B.; Slater, D. R.; Whalen, K. L. Enzyme Function Initiative-Enzyme Similarity Tool (EFI-EST): A Web Tool for Generating Protein Sequence Similarity Networks. *Biochimica et Biophysica Acta - Proteins and Proteomics* **2015**, *1854* (8), 1019−1037.
(39) Macdonald, S. S.; Armstrong, Z.; Morgan-Lang, C.; Osowiecka, M.; Robinson, K.; Hallam, S. J.; Withers, S. G. Development and Application of a High-Throughput Functional Metagenomic Screen for Glycoside Phosphorylases. *Cell Chemical Biology* **2019**, *26* (7), 1001−1012.
(40) Lazarev, V. N.; Levitskii, S. A.; Basovskii, Y. I.; Chukin, M. M.; Akopian, T. A.; Vereshchagin, V. V.; Kostrjukova, E. S.; Kovaleva, G. Y.; Kazanov, M. D.; Malko, D. B.; et al. Complete Genome and Proteome of Acholeplasma Laidlawii. *J. Bacteriol.* **2011**, *193* (18), 4943−4953.
(41) De Groeve, M. R. M.; Tran, G. H.; Van Hoorebeke, A.; Stout, J.; Desmet, T.; Savvides, S. N.; Soetaert, W. Development and Application of a Screening Assay for Glycoside Phosphorylases. *Anal. Biochem.* **2010**, *401* (1), 162−167.
(42) Kuhaudomlarp, S.; Patron, N. J.; Henrissat, B.; Rejzek, M.; Saalbach, G.; Field, R. A. Identification of Euglena Gracilis β-1,3-Glucan Phosphorylase and Establishment of a New Glycoside Hydrolase (GH) Family GH149. *J. Biol. Chem.* **2018**, *293* (8), 2865−2876.
(43) Cai, L.; Guan, W.; Kitaoka, M.; Shen, J.; Xia, C.; Chen, W.; Wang, P. G. A Chemoenzymatic Route to N-Acetylglucosamine-1-Phosphate Analogues: Substrate Specificity Investigations of N-Acetylhexosamine 1-Kinase. *Chem. Commun.* **2009**, No. 20, 2944.
(44) Eddenden, A.; Kitova, E. N.; Klassen, J. S.; Nitz, M. An Inactive Dispersin B Probe for Monitoring PNAG Production in Biofilm Formation. *ACS Chem. Biol.* **2020**, *15* (5), 1204−1211.

https://doi.org/10.1021/acscentsci.1c01570
ACS Cent. Sci. XXXX, XXX, XXX−XXX

(45) Robbins, P. W.; Overbye, K.; Albright, C.; Benfield, B.; Pero, J. Cloning and High-Level Expression of Chitinase-Encoding Gene of Streptomyces Plicatus. *Gene* **1992**, *111* (1), 69−76.
(46) Mark, B. L.; Wasney, G. A.; Salo, T. J. S.; Khan, A. R.; Cao, Z.; Robbins, P. W.; James, M. N. G.; Triggs-Raine, B. L. Structural and Functional Characterization of Streptomyces Plicatus β-N-Acetylhexosaminidase by Comparative Molecular Modeling and Site-Directed Mutagenesis. *J. Biol. Chem.* **1998**, *273* (31), 19618−19624.
(47) Williams, S. J.; Mark, B. L.; Vocadlo, D. J.; James, M. N. G.; Withers, S. G. Aspartate 313 in the Streptomyces PlicatusHexosaminidase Plays a Critical Role in Substrate-Assisted Catalysis by Orienting the 2-Acetamido Group and Stabilizing the Transition State. *J. Biol. Chem.* **2002**, *277* (42), 40055−40065.
(48) Kudelka, M. R.; Ju, T.; Heimburg-Molinaro, J.; Cummings, R. D. Simple Sugars to Complex Disease–Mucin-Type O-Glycans in Cancer. *Advances in cancer research* **2015**, *126* (1), 53−135.
(49) Koutsioulis, D.; Landry, D.; Guthrie, E. P. Novel Endo-α-N-Acetylgalactosaminidases with Broader Substrate Specificity. *Glycobiology* **2008**, *18* (10), 799−805.
(50) Berman, H. M.; Westbrook, J.; Feng, Z.; Gilliland, G.; Bhat, T. N.; Weissig, H.; Shindyalov, I. N.; Bourne, P. E. The Protein Data Bank. *Nucleic acids research* **2000**, *28* (1), 235−242.
(51) Hidaka, M.; Honda, Y.; Kitaoka, M.; Nirasawa, S.; Hayashi, K.; Wakagi, T.; Shoun, H.; Fushinobu, S. Chitobiose Phosphorylase from Vibrio Proteolyticus, a Member of Glycosyl Transferase Family 36, Has a Clan GH-L-like (α/α)6 Barrel Fold. *Structure* **2004**, *12* (6), 937−947.
(52) Macdonald, S. S.; Patel, A.; Larmour, V. L. C.; Morgan-Lang, C.; Hallam, S. J.; Mark, B. L.; Withers, S. G. Structural and Mechanistic Analysis of a β-Glycoside Phosphorylase Identified by Screening a Metagenomic Library. *J. Biol. Chem.* **2018**, *293* (9), 3451−3467.
(53) Petersen, L.; Ardèvol, A.; Rovira, C.; Reilly, P. J. Mechanism of Cellulose Hydrolysis by Inverting GH8 Endoglucanases: A QM/MM Metadynamics Study. *J. Phys. Chem. B* **2009**, *113* (20), 7331−7339.
(54) Davies, G. J.; Planas, A.; Rovira, C. Conformational Analyses of the Reaction Coordinate of Glycosidases. *Accounts of chemical research* **2012**, *45* (2), 308−316.
(55) Laidlaw, P. P.; Elford, W. J. A New Group of Filterable Organisms. *Proceedings of the Royal Society of London. Series B - Biological Sciences* **1936**, *120* (818), 292−303.
(56) Windsor, H. M.; Windsor, G. D.; Noordergraaf, J. H. The Growth and Long Term Survival of Acholeplasma Laidlawii in Media Products Used in Biopharmaceutical Manufacturing. *Biologicals* **2010**, *38* (2), 204−210.
(57) Chernov, V. M.; Mouzykantov, A. A.; Baranova, N. B.; Medvedeva, E. S.; Grygorieva, T. Y.; Trushin, M. V.; Vishnyakov, I. E.; Sabantsev, A. V.; Borchsenius, S. N.; Chernova, O. A. Extracellular Membrane Vesicles Secreted by Mycoplasma Acholeplasma Laidlawii PG8 Are Enriched in Virulence Proteins. *Journal of Proteomics* **2014**, *110*, 117−128.
(58) Volokhov, D. V.; Graham, L. J.; Brorson, K. A.; Chizhikov, V. E. Mycoplasma Testing of Cell Substrates and Biologics: Review of Alternative Non-Microbiological Techniques. *Molecular and Cellular Probes* **2011**, *25* (2−3), 69−77.
(59) Chernov, V. M.; Chernova, O. A.; Mouzykantov, A. A.; Baranova, N. B.; Gorshkov, O. V.; Trushin, M. V.; Nesterova, T. N.; Ponomareva, A. A. Extracellular Membrane Vesicles and Phytopathogenicity of Acholeplasma Laidlawii PG8. *Scientific World Journal* **2012**, *2012*, 1−6.
(60) Marcone, C. Molecular Biology and Pathogenicity of Phytoplasmas. *Annals of Applied Biology* **2014**, *165* (2), 199−221.
(61) Gilliam, J. M.; Morowitz, H. J. Characterization of the Plasma Membrane of Mycoplasma Laidlawii. *Biochimica et Biophysica Acta (BBA) - Biomembranes* **1972**, *274* (2), 353−363.
(62) Terry, T. M.; Zupnik, J. S. Weak Association of Glucosamine-Containing Polymer with the Acholeplasma Laidlawii Membrane. *BBA - Biomembranes* **1973**, *291* (1), 144−148.
(63) McElhaney, R. N. The Structure and Function of the Acholeplasma Laidlawii Plasma Membrane. *BBA - Reviews on Biomembranes* **1984**, *779* (1), 1−42.
(64) Welner, D. H.; Shin, D.; Tomaleri, G. P.; DeGiovanni, A. M.; Yi-Lin Tsai, A.; Tran, H. M.; Hansen, S. F.; Green, D. T.; Scheller, H. v.; Adams, P. D. Plant Cell Wall Glycosyltransferases: High-Throughput Recombinant Expression Screening and General Requirements for These Challenging Enzymes. *PLoS One* **2017**, *12* (6), No. e0177591.

https://doi.org/10.1021/acscentsci.1c01570
ACS Cent. Sci. XXXX, XXX, XXX−XXX